European Review for Medical and Pharmacological Sciences 2020; 24: 3245-3253

Effect of miR-126 on intracranial aneurysms and its predictive value for rupture of aneurysms

F. YANG[1], W.-W. XING[2], D.-W. SHEN[3], M.-F. TONG[1], F.-M. XIE[4]

[1]Department of Neurosurgery, Jinhua Municipal Central Hospital, Jinhua, P.R. China
[2]Department of Pediatrics, Yidu Central Hospital of Weifang, Weifang, P.R. China
[3]Department of Neurosurgery, Yidu Central Hospital of Weifang, Weifang, P.R. China
[4]Department of Neurosurgery, The Second Affiliated Hospital of Shandong First Medical University, Shandong First Medical University and the Shandong Academy of Medical Sciences, Taian, P.R. China

Abstract. – OBJECTIVE: This study aimed to investigate the effect of miR-126 on intracranial aneurysm (IA) and its predictive value for aneurysm rupture.

PATIENTS AND METHODS: Altogether 102 patients (patient group) with IA diagnosed in the Jinhua Municipal Central Hospital from July 2016 to April 2018, and 80 healthy people (normal group) who underwent physical examination during the same period were collected. QRT-PCR was used to detect the expression of miR-126 in serum, analyze the expression of miR-126 in IA, and explore the predictive value on IA rupture. Potential target genes of miR-126 were analyzed by target gene prediction website, and David was used to analyze the enrichment of miR-126 target gene GO and KEGG.

RESULTS: The expression of miR-126 in serum of patient group was significantly higher than that of normal group ($p < 0.05$), ROC curve area was 0.966. The high expressions of miR-126 were directly related to the possibility of large lesions ($p < 0.05$). Multivariate analysis showed that lesion size and miR-126 expression were independent risk factors for rupture of IA patients. ROC curve showed that lesion size and miR-126 expression area under the curve were 0.707 and 0.827. Altogether 520 potential target sites were found by Venn diagram of Targetscan, miRDB, and Starbase online miR-126 prediction website. GO enrichment and KEGG analysis by David online software found that miR-126 target genes were mainly enriched in 169 biological processes, such as nucleus, transcription, DNA-templated, transcription factor activity, sequence-specific DNA binding, protein binding, and phosphatidylinositol phosphorylation. KEGG analysis found that miR-126 target genes were significantly enriched in MAPK signaling pathway, pathways in cancer, ErbB signaling pathway, MicroRNAs in cancer, and Thyroid hormone signaling pathway.

CONCLUSIONS: MiR-126 can be used as a potential diagnostic and predictive indicator for IA occurrence and IA rupture.

Key Words:
MiR-126, Intracranial aneurysm, GO enrichment, KEGG enrichment.

Introduction

Intracranial aneurysm (IA) is a common hemorrhagic cerebrovascular disease in clinical practice[1]. Studies[2] showed that IA has the possibility of occurrence at any age, but it is mostly found in women aged 40 to 60 years. Hop et al[3] showed that the incidence rate of patients with aneurysm rupture and hemorrhage is 3-17.8/100,000, but the risk of IA rupture and hemorrhage is about 1%. Most IA patients have no evident clinical symptoms before rupture occurs. Once rupture occurs, patients may suffer from subarachnoid hemorrhage. In light cases, limb dysfunction may occur, and in heavy cases, the life of patients may be endangered[4]. At present, the mechanism of formation and rupture of IA is not clinically clear. Most scholars believed that the occurrence and rupture of IA are closely related to hemodynamics and arterial wall structure[5], so it is particularly important to find out the mechanism of IA.

MicroRNA (miR) is a short-chain non-coding RNA with a length of about 21-25nt, which is highly conservative[6]. Hoffman et al[7] and Rouleau et al[8] have shown that miR can regulate protein expression by regulating Untranslated Regions (UTR) at the 3' end of downstream target gene mRNA for complete or incomplete binding and complementation, thus affecting mRNA stability or inhibiting its translation. Meeuwsen[9] have shown that miR is involved in the development of IA. Luo et al[10] found that miR-9 over-expression can inhibit proliferation, reduce contractility of

Corresponding Author: Fangmin Xie, MD; e-mail: 1977_1@sina.com

smooth muscle cells, and promote the development of intracranial aneurysms. Sun et al[11] found that miR-29b downregulation induces phenotypic regulation of vascular smooth muscle cells, which may be a potential reason for IA formation. Moreover, Jin et al[12] have shown that miRs is a new potential biomarker and can be used for early diagnosis of intracranial aneurysm rupture. As a member of miR family, Salajegheh et al[13] have found that miR-126 is related to the occurrence and development of various tumors and can directly target vascular endothelial growth factor (VEGF) to regulate tumor proliferation. VEGF is an important vascular growth factor. Liu et al[14] have shown that inflammatory smooth muscle cells affect the progress of IA by regulating VEGF expression and inducing endothelial cell changes. Therefore, we speculated that miR-126 may also be involved in the development of IA. However, there is little research on miR-126 in IA at present.

This study aimed to analyze the expression and clinical value of miR-126 in IA through bioinformatics and clinical research to provide potential targets for future treatment.

Patients and Methods

Sample Data Collection

Altogether 102 patients with IA diagnosed in the Jinhua Municipal Central Hospital from July 2016 to April 2018 were collected as patient group, including 79 patients with IA rupture (ruptured group), 23 patients without IA rupture (unruptured group), and 80 healthy people who underwent physical examination during the same period were collected as normal group. This investigation was approved by the Medical Ethics Committee of Jinhua Municipal Central Hospital. Inclusion criteria were as follows: patients were diagnosed as IA through imaging examination; patients had not been treated with IA therapy before this study; patients had less than 1 lesion; patients had complete clinical data, and the patients or their families signed informed consent form. Exclusion criteria were as follows: patients were diagnosed as secondary IA; patients with cystic aneurysm; patients with severe cardiac, hepatic and renal insufficiency; pregnant women.

Sample Collection and Detection

A 5 ml of peripheral venous blood from two groups of people were collected, placed for 30 min, centrifuged at 3000 rpm for 10 min. The supernatant was then collected for total RNA extraction, and the total RNA in serum was extracted using TRIzol (Invitrogen, Carlsbad, CA, USA, 15596018). The purity, concentration, and integrity of the total RNA after extraction were detected using ultraviolet spectrophotometer and agarose gel electrophoresis. TransScript® miRNA RT Enzyme Mix and 2×TS miRNA Reaction Mix from TransScript Green miRNA Two-Step qRT-PCR SuperMix (TransGen Biotech, Beijing, China, AQ202-01) were used to reverse transcribe the total RNA. The operation steps were strictly in accordance with the manufacturer's kit. The cDNA was collected, and PCR was amplified using ABI 7500 PCR instrument (Applied Biosystems, Foster City, CA, USA, 7500). The upstream sequence of miR-126 was 5'-GTCGTATCCAGTGCAGGGTCCGAG-3', the downstream sequence was 5'-GTATTCGCACTGGATACGAC-3'. The upstream sequence of U6 was 5'-CTCGCTTCGGCAGCACA-3', and the downstream sequence was 5'-AACGCTTCACGAATTTGCGT-3'. The amplification reaction system was as follows: 1 μL of cDNA, 0.4 μL of upstream and downstream primers, 10 μl of 2×TransTaq® Tip Green qPCR SuperMix, 0.4 μL of Passive Reference Dye (50x), and finally ddH2O was added to make up to 20 μL. The amplification reaction conditions were as follows: pre-denaturation at 94°C for 30 s, denaturation at 94°C for 5 s, annealing at 60°C for 30 s, and a total of 40 cycles. Each sample was provided with 3 repeated wells, and the experiment was carried out 3 times. U6 was used as internal reference, and $2^{-\Delta ct}$ was used to analyze the data.

Bioinformatics Analysis

Targetscan, miRDB, and Starbase were used to predict the potential target genes of miR-126 and visualize a Venn diagram. David online software was used to enrich GO and KEGG for the common target genes predicted by the three websites to find the potential influence function and signal pathway of miR-126.

Statistical Analysis

SPSS 20.0 software package was used for statistical analysis of the collected data. GraphPad 7 software package was used to visualize the required graphs. K-S test was used to analyze the distribution of dose data. Normal distribution data was expressed by mean± standard deviation (Meas± SD). Inter-group comparison

was expressed by independent sample *t*-test, counting data was expressed by utilization (%) and analyzed by Chi-square test (denoted by χ^2). One-way ANOVA was used for comparison among multiple groups, which was expressed as F. Least Significant Difference (LSD) *t*-test was used for subsequent pairwise comparisons, ROC was used to plot the diagnostic value of miR-126 in IA, and Logistic regression was used to analyze the independent risk factors of IA rupture. The *p*-value less than 0.050 was statistically significant.

Results

Baseline Data of Patients

Comparing the clinical data of the two groups of patients, it was found that there was no statistical difference between the two groups in sex, age, BMI, smoking history, and residence ($p > 0.05$) (Table I).

Expression and Clinical Value of MiR-126 in IA Patients

Comparing the expression of miR-126 in the serum of the patient group with that of normal group, it was found that the expression of miR-126 in the serum of patient group was significantly increased, and the area of miR-126 under the diagnosis curve of IA patients was 0.966 by ROC curve analysis. Furthermore, patients were divided into high and low expression groups according to the median value of miR-126. The relation between miR-126 and clinical data of patients was analyzed. It was found that higher expressions of miR-126 were directly related to the possibility of large lesions ($p < 0.05$) (Table II and Figure 1).

Analysis of Risk Factors for IA Rupture

Patients were divided into two groups, according to the IA rupture condition. Comparing the clinical data of ruptured group with unruptured group, it was found that the age, smoking history, lesion size, and miR-126 expression were risk factors affecting IA rupture. Therefore, we further included the indicators with differences and took rupture condition as independent variable after assignment (see Table IV). The multi-factor analysis using the Lagrangian Relaxation (LR) method showed that the lesion size and miR-126 expression were independent risk factors for IA patients rupture. Furthermore, the ROC curve was visualized for the indicators with multi-factor significance. It was found that the lesion size and the area under the miR-126 expression curve were 0.707 and 0.827, which had high diagnostic value (Table III, IV, V, and Figure 2).

Table I. Baseline data.

Factor		Patient group (n=102)	Control group (n=80)	χ^2/*t*-value	*p*-value
Sex				0.233	0.629
	Male	41 (40.20)	35 (43.75)		
	Female	61 (59.80)	45 (56.25)		
Age (years)		53.6 ± 4.9	52.8 ± 4.0	1.183	0.238
BMI (kg/m^2)		22.47 ± 2.54	22.08 ± 1.88	1.148	0.252
Smoking history				0.041	0.839
	Yes	50 (49.02)	38 (47.50)		
	No	52 (50.98)	42 (52.50)		
Drinking history				0.184	0.668
	Yes	15 (14.71)	10 (12.50)		
	No	87 (85.29)	70 (87.50)		
Residence				0.861	0.354
	Urban	80 (78.43)	58 (72.50)		
	Rural	22 (21.57)	22 (27.50)		
Lesion location					
	Anterior artery	70 (68.63)			
	Posterior artery	32 (31.37)			
Lesion size					
	< 5 mm	56 (54.90)			
	5-10mm	27 (26.47)			
	> 10 mm	19 (18.63)			

Table II. Analysis of miR-125 and baseline data of IA patients.

Factor		MiR-126 expression		χ^2/Z value	*p*-value
		High-expression (n = 51)	Low-expression (n = 51)		
Sex				1.020	0.313
	Male (n = 41)	23 (45.10)	18 (35.29)		
	Female (n = 61)	28 (54.90)	33 (64.71)		
Age (years)				2.558	0.120
	< 55 (n = 58)	25 (49.02)	33 (64.71)		
	≥ 55 (n = 44)	26 (50.98)	18 (35.29)		
BMI (kg/m^2)				0.355	0.551
	< 22 (n = 47)	25 (49.02)	22 (43.14)		
	≥ 22 (n = 55)	26 (50.98)	29 (56.86)		
Smoking history				0.157	0.692
	Yes (n = 50)	24 (47.06)	26 (49.02)		
	No (n = 52)	27 (51.92)	25 (50.98)		
Drinking history				0.703	0.402
	Yes (n = 15)	9 (17.65)	6 (11.76)		
	No (n = 87)	42 (82.35)	45 (88.24)		
Residence				0.927	0.336
	Urban (n = 80)	42 (82.35)	38 (74.51)		
	Rural (n = 22)	9 (17.65)	13 (25.49)		
Lesion location				1.639	0.200
	Anterior artery (n = 70)	38 (74.51)	32 (62.75)		
	Posterior artery (n = 32)	13 (25.49)	19 (37.25)		
Lesion size				-2.837	0.005
	< 5 mm (n = 56)	19 (37.25)	37 (71.15)		
	5-10 mm (n = 27)	21 (41.18)	6 (11.54)		
	> 10 mm (n = 19)	11 (21.57)	9 (17.31)		

Bioinformatics Analysis

Altogether 520 potential target sites were found by Venn diagram of Targetscan, miRDB, and Starbase online miR-126 prediction. GO enrichment and KEGG analysis by the David online software found that miR-126 target genes were mainly enriched in 169 biological processes, such as nucleus, transcription, DNA-templated, transcription factor activity, sequence-specific DNA binding, protein binding, and phosphatidylinosi-

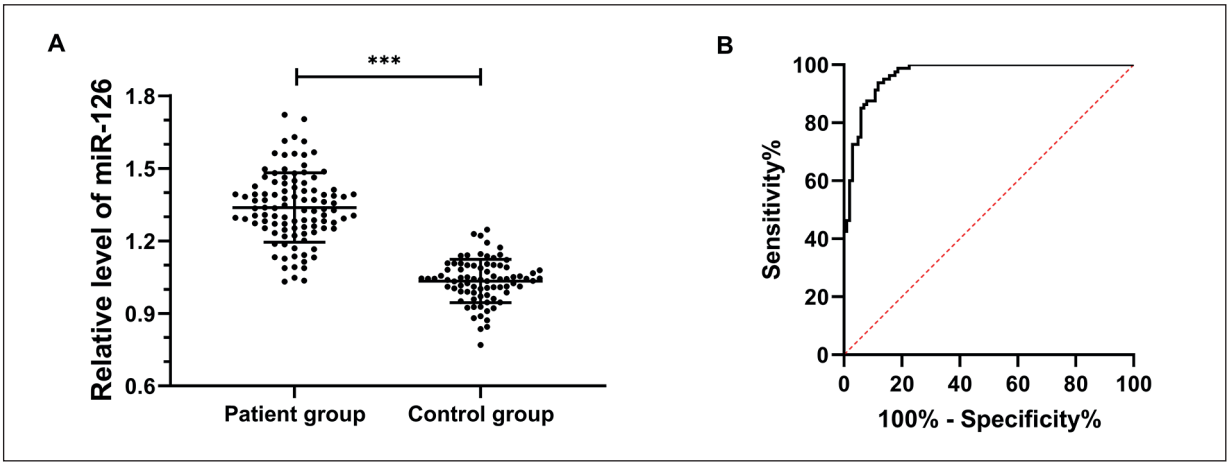

Figure 1. Expression and diagnostic value of mir-126 in IA. **A,** MiR-126 is highly expressed in IA patients. **B,** The diagnostic value of miR-126 in IA patients. When the cut-off value is 1.155, the optimal specificity is 88.24%, sensitivity is 93.75%, and Youden index is 81.99%.

Table III. Single factor analysis.

Factor		Ruptured group (n = 79)	Unruptured group (n = 23)	χ^2/Z value	*p*-value
Sex				0.719	0.396
	Male (n = 41)	30 (37.97)	11 (47.83)		
	Female (n = 61)	49 (62.03)	12 (52.17)		
Age (years)				5.343	0.019
	< 55 (n = 58)	40 (50.63)	18 (78.26)		
	≥ 55 (n = 44)	39 (49.37)	5 (21.74)		
BMI (kg/m^2)				2.615	0.106
	< 22 (n = 47)	33 (41.77)	14 (60.87)		
	≥ 22 (n = 55)	46 (58.64)	9 (39.13)		
Smoking history				3.888	0.049
	Yes (n = 50)	43 (53.75)	7 (30.43)		
	No (n = 52)	37 (46.25)	16 (69.57)		
Drinking history				1.171	0.279
	Yes (n = 15)	10 (12.66)	5 (21.74)		
	No (n = 87)	69 (87.34)	18 (78.26)		
Residence				0.358	0.549
	Urban (n = 80)	63 (79.75)	17 (73.91)		
	Rural (n = 22)	16 (20.25)	6 (26.06)		
Lesion location				3.734	0.053
	Anterior artery (n = 70)	58 (73.42)	12 (52.17)		
	Posterior artery (n = 32)	21 (26.58)	11 (47.83)		
Lesion size				-2.082	0.037
	< 5 mm (n = 56)	39 (49.37)	17 (73.91)		
	5-10 mm (n = 27)	23 (29.11)	4 (17.39)		
	> 10 mm (n = 19)	17 (21.52)	2 (8.70)		
miR-126 expression				6.793	0.009
	High-expression (n=51)	45 (56.96)	6 (26.09)		
	Low-expression (n=51)	34 (43.04)	17 (73.91)		

tol phosphorylation. KEGG analysis found that miR-126 target genes were significantly enriched in 44 pathways, such as MAPK signaling pathway, Pathways in cancer, ErbB signaling pathway, MicroRNAs in cancer, and Thyroid hormone signaling pathway (Figure 3, Table VI and VII).

Discussion

MiR is a short-chain non-coding RNA, which can change the expression by targeting the target gene and controlling the biotransformation process[15]. In recent years, several research reports showed that miR and IA are closely related. In the research of Wang et al[16], miR-29 was found to be a potential biomarker for IA occurrence. However, in the research of Zhang et al[17], miR-448-3p was found to control IA by regulating KLF5 expression, miR-126 was located on human 9q34.3 chromosome. Previous investigations[18] on miR were mostly in tumor direction, while studies on IA were few.

In this study, we detected the expression of miR-126 in serum of patients with IA and normal people, and found that the expression of miR-126 in patients with IA increased significantly, which indicated that miR-126 was expected to become a potential diagnostic indicator for IA. Therefore, we further visualized ROC curve, and found that the area under the curve was more than 0.95, which indicated that miR-126 had a very high clinical diagnostic value in diagnosing IA. Kong et al[19] found that miR-126 can target VEGF-A to inhibit esophageal cancer. However, in the research of Chen et al[20], it was found that reduction

Table IV. Assignment table.

Factor	Assignment
Age	< 55 = 1, ≥ 55 =2
Smoking history	Yes = 1, No = 2
Lesion size	< 5 mm = 1, 5-10 mm = 2, > 10 mm = 3
miR126 expression	High expression = 1, Low expression = 2

Table V. Multivariate analysis.

Factor	β	SD	χ^2	*p*	OR	95% CI	
						Lower limit	Superior limit
Age	0.350	0.518	0.457	0.499	1.420	0.514	3.920
Smoking history	-1.017	0.536	3.596	0.058	0.362	0.126	1.035
Lesion size	0.766	0.388	3.893	0.048	2.150	1.005	4.600
miR126 expression	-1.257	0.547	5.275	0.022	0.284	0.097	0.832

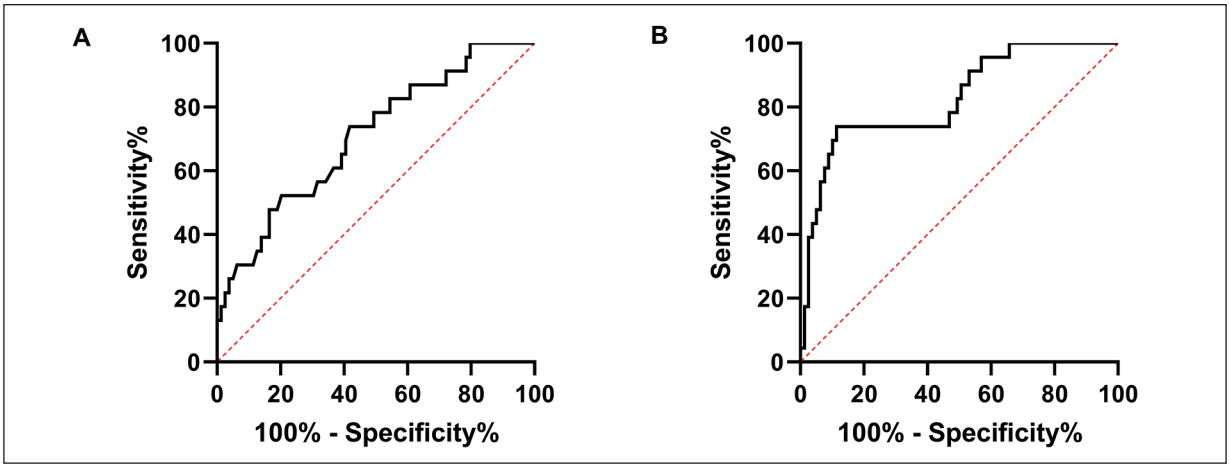

Figure 2. Predictive value of lesion size and miR-126 expression for IA rupture. **A,** Predictive value curve of lesion size for IA rupture. When the cut-off value is 4.606mm, the optimal specificity is 58.23%, sensitivity is 73.91%, and Youden index is 32.14%. **B,** Predictive Value Curve of miR-126 for IA rupture. When the cut-off value of miR-126 for predicting IA rupture is 1.252, the optimal specificity is 88.60%, sensitivity is 73.91%, and Youden index is 62.52%.

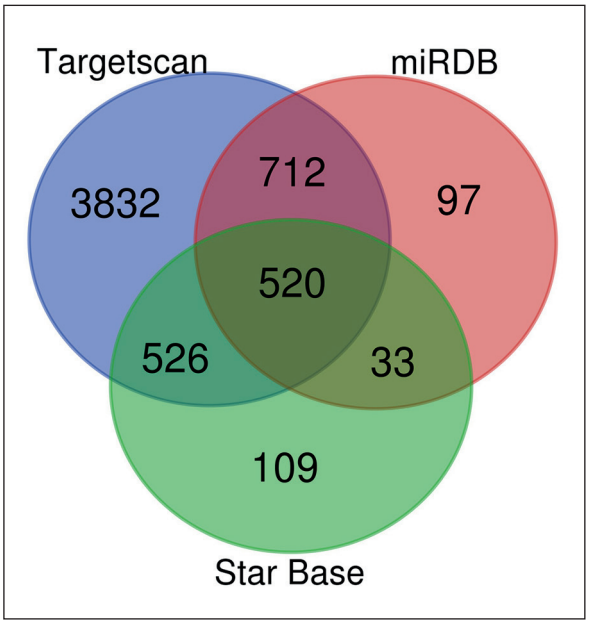

Figure 3. Venn diagram. Blue part is the potential target gene predicted by TargetScan website, red part is the potential target gene predicted by miRDB website, and green part is the potential target gene predicted by StarBase website.

of miR-126 may regulate angiogenesis of gastric cancer induced by vascular endothelial growth factor-A (VEGF-A). VEGF is an important factor in angiogenesis. Li et al[21] have shown that VEGF participates in the occurrence of IA, and miR-126 can be used as an upstream gene that can regulate VEGF. Therefore, we speculate that miR-126 is closely related to IA. We have verified through detection that miR-126 has differential expression in IA. Moreover, we further analyzed the relation between miR-126 and clinical data according to the high expression of miR-126. The results showed that the number of patients with lesions larger than 10 mm in patients with high expression of miR-126 was significantly increased, which suggested that miR-126 was related to the lesion size of patients. Therefore, we speculated that this is related to the increased expression of miR-126, which promotes angiogenesis and enlarges the lesions.

Due to abnormal lesion of the intracranial vessel wall, the AI lesion is generally fusiform or cystic types[22]. Juvela and Korja[23] have found

Table VI. Enrichment of miR-126 target gene GO.

GO number	GO note	Gene dosage [n(%)]	p	Gene
0005634	Nucleus	200 (38.46)	2.93E-07	ITGB3BP, PTGS2, CHMP5, RORA, ZNF254
0006351	Transcription, DNA-templated	90 (17.31)	5.09E-06	ITGB3BP, CCNT2, ZNF81, GPBP1, E2F7
0003700	Transcription factor activity, sequence-specific DNA binding	51 (9.81)	1.60E-05	ZNF81, GPBP1, E2F7, MITF, RORA
0005515	Protein binding	290 (55.77)	2.26E-05	ITGB3BP, VAPA, PTGS2, C16ORF72, CHMP5
0046854	Phosphatidylinositol phosphorylation	12 (2.31)	7.55E-05	FGFR2, IMPAD1, FGF7, EREG, GRB2

that more than 75.00% of subarachnoid hemorrhage is caused by IA rupture, and IA has no evident clinical features before rupture, which is also called "invisible killer" clinically. Therefore, early diagnosis and treatment are effective means to prevent IA rupture. With the continuous improvement of imaging technology, spontaneous subarachnoid hemorrhage caused by IA rupture has been effectively treated. However, there is currently a lack of predictive indicators for IA rupture. In this study, we further divided the patients according to IA rupture. Through multivariate analysis, we found that lesion size and miR-126 expression are independent risk factors for IA rupture in patients. Mocco et al[24] have proved that lesion size is an independent risk factor for IA rupture. In this present study, we discovered for the first time that miR-126 can also be an independent risk factor for IA rupture. Moreover, we found that both indexes have high value in predicting IA rupture by ROC curve, and the area under miR-126 curve is obviously larger than the lesion size, which also showed that miR-126 expression has high diagnostic value in predicting IA rupture. However, we are still not clear about its relevant mechanism. Therefore, we have carried out prediction of miR-126 target genes and enrichment of GO and KEGG. Through enrichment results of GO and KEGG, we found that miR-126 target genes are mainly enriched in biological functions, such as nucleus, transcription, DNA-templated, transcription factor activity, sequence-specific DNA binding, protein binding, and phosphatidylinositol phosphorylation, etc. However, KEGG enrichment found that miR-126 target genes were enriched in the MAPK signaling pathway, Pathways in cancer, ErbB signaling pathway, MicroRNAs in cancer, Thyroid hormone signaling pathway, and other pathways. It is worth noting that the MAPK signaling pathway is expressed in a variety of vascular cells, including vascular endothelial cells, vascular smooth muscle cells, and can also regulate vascular signal transduction pathway[25]. We speculate that miR-126 may regulate the occurrence of IA through the MAPK signaling pathway, which is also the main direction of our future research.

Table VII. Enrichment analysis of miR-126 target gene KEGG.

KEGG pathway	Gene dosage [n(%)]	p	Gene
MAPK signaling pathway	18 (3.46)	1.17E-04	PRKCA, FGFR2, LAMTOR3, FGF7, GRB2
Pathways in cancer	22 (4.23)	4.63E-04	PRKCA, FGFR2, DVL3, FGF7, ROCK1
ErbB signaling pathway	9 (1.73)	0.001123526	PRKCA, KRAS, CRKL, EREG, GRB2
MicroRNAs in cancer	17 (3.27)	0.001407331	RECK, PRKCA, ROCK1, PTGS2, GRB2
Thyroid hormone signaling pathway	10 (1.92)	0.001760596	PRKCA, KAT2B, KRAS, HIF1A, MED17

In this report, we determined that miR-126 can be used as a potential diagnostic index for IA and a predictive index for judging IA rupture by detecting the expression of miR-126 in serum of IA patients. However, our study still has certain limitations. First, we have not carried out relevant basic research as a clinical study. Second, we have not carried out short-term follow-up of patients. Whether miR-126 affects the prognosis of patients' needs further investigation. Finally, as the samples in this study are all Asian patients, it is unclear whether miR-126 has the same predictive value in other races. Therefore, we hope to collect more samples of different types of people in future research, and conduct follow-up and basic research to address the deficiencies of our research.

Conclusions

Briefly, we showed that miR-126 could be used as a potential diagnostic and predictive indicator for IA occurrence and IA rupture.

Conflict of Interest

The Authors declare that they have no conflict of interests.

Acknowledgements

This study was supported by New Techniques of Craniotomy and Standardized Diagnosis and Treatment of Anterior Circulation Aneurysm of Provincial Key Research and Development Project (No. 2019C03044).

References

1) Cebral J, Ollikainen E, Chung BJ, Mut F, Sippola V, Jahromi BR, Tulamo R, Hernesniemi J, Niemelä M, Robertson A, Frösen J. Flow conditions in the intracranial aneurysm lumen are associated with inflammation and degenerative changes of the aneurysm wall. AJNR Am J Neuroradiol 2017; 38: 119-126.
2) Rouchaud A, Brandt MD, Rydberg AM, Kadirvel R, Flemming K, Kallmes DF, Brinjikji W. Prevalence of intracranial aneurysms in patients with aortic aneurysms. AJNR Am J Neuroradiol 2016; 37: 1664-1668.
3) Hop JW, Rinkel GJ, Algra A, van Gijn J. Case-fatality rates and functional outcome after subarachnoid hemorrhage: a systematic review. Stroke 1997; 28: 660-664.
4) Zhang WH, Qiao CH, Zhang X, Luo H, Sun XK. The expression of MMP-7 in serum and aneurysm tissues of patients with abdominal aortic aneurysm associated with hypertension and the clinical efficacy of endovascular exclusion. Eur Rev Med Pharmacol Sci 2017; 21: 4623-4631.
5) Khan MO, Valen-Sendstad K, Steinman DA. Narrowing the expertise gap for predicting intracranial aneurysm hemodynamics: impact of solver numerics versus mesh and time-step resolution. AJNR Am J Neuroradiol 2015; 36: 1310-1316.
6) Agarwal V, Bell GW, Nam JW, Bartel DP. Predicting effective microRNA target sites in mammalian mRNAs. eLife 2015; 4. doi: 10.7554/eLife.05005.
7) Hoffman Y, Bublik DR, Ugalde AP, Elkon R, Biniashvili T, Agami R, Oren M, Pilpel Y. 3'UTR shortening potentiates microRNA-based repression of pro-differentiation genes in proliferating human cells. PLoS Genet 2016; 12: e1005879.
8) Rouleau S, Glouzon JS, Brumwell A, Bisaillon M, Perreault JP. 3′ UTR G-quadruplexes regulate miRNA binding. RNA 2017; 23: 1172-1179.
9) Meeuwsen JAL, van T Hof FNG, van Rheenen W, Rinkel GJE, Veldink JH, Ruigrok YM. Circulating microRNAs in patients with intracranial aneurysms. PLoS One 2017; 12: e0176558.
10) Luo J, Jin H, Jiang Y, Ge H, Wang J, Li Y. Aberrant expression of microRNA-9 contributes to development of intracranial aneurysm by suppressing proliferation and reducing contractility of smooth muscle cells. Med Sci Monit 2016; 22: 4247-4253.
11) Sun L, Zhao M, Zhang J, Lv M, Li Y, Yang X, Liu A, Wu Z. MiR-29b downregulation induces phenotypic modulation of vascular smooth muscle cells: implication for intracranial aneurysm formation and progression to rupture. Cell Physiol Biochem 2017; 41: 510-518.
12) Jin H, Li C, Ge H, Jiang Y, Li Y. Circulating microRNA: a novel potential biomarker for early diagnosis of intracranial aneurysm rupture a case control study. J Transl Med 2013; 11: 296.
13) Salajegheh A, Vosgha H, Rahman MA, Amin M, Smith RA, Lam AK. Interactive role of miR-126 on VEGF-A and progression of papillary and undifferentiated thyroid carcinoma. Hum Pathol 2016; 51: 75-85.
14) Liu P, Shi Y, Fan Z, Zhou Y, Song Y, Liu Y, Yu G, An Q, Zhu W. Inflammatory smooth muscle cells induce endothelial cell alterations to influence cerebral aneurysm progression via regulation of integrin and VEGF expression. Cell Transplant 2019; 28: 713-722.
15) Wang JQ, Gu WP, Deng QQ, Huang Q, Wang AM, Liu SX, Tang HY, Liang Y, Yan JH, Ouyang S. Endothelial progenitor cell miR-126 promotes homing of endothelial progenitor cells within arterial thrombus in patients with cerebral infarction and its molecular mechanism. Eur Rev Med Pharmacol Sci 2018, 22: 1078-1083.
16) Wang WH, Wang YH, Zheng LL, Li XW, Hao F, Guo D. MicroRNA-29a: a potential biomarker in the development of intracranial aneurysm. J Neurol Sci 2016; 364: 84-89.

17) Zhang JZ, Chen D, Lv LQ, Xu Z, Li YM, Wang JY, Han KW, Yu MK, Huang CG, Hou LJ. MiR-448-3p controls intracranial aneurysm by regulating KLF5 expression. Biochem Biophys Res Commun 2018; 505: 1211-1215.

18) Lin S, Gregory RI. MicroRNA biogenesis pathways in cancer. Nature Rev Cancer 2015; 15: 321-333.

19) Kong R, Ma Y, Feng J, Li S, Zhang W, Jiang J, Zhang J, Qiao Z, Yang X, Zhou B. The crucial role of miR-126 on suppressing progression of esophageal cancer by targeting VEGF-A. Cell Mol Biol Lett 2016; 21: 3.

20) Chen H, Li L, Wang S, Lei Y, Ge Q, Lv N, Zhou X, Chen C. Reduced miR-126 expression facilitates angiogenesis of gastric cancer through its regulation on VEGF-A. Oncotarget 2014; 5: 11873-11885.

21) Li T, Wang H, Li X, Ge H, Sun H, Ma D. Predictive significance of VEGFA variations in intracranial aneurysm. Int J Clin Exp Med 2017; 10: 13802-13807.

22) Murayama Y, Takao H, Ishibashi T, Saguchi T, Ebara M, Yuki I, Arakawa H, Irie K, Urashima M, Molyneux AJ. Risk analysis of unruptured intracranial aneurysms: prospective 10-year cohort study. Stroke 2016; 47: 365-371.

23) Juvela S, Korja M. Intracranial aneurysm parameters for predicting a future subarachnoid hemorrhage: a long-term follow-up study. Neurosurgery 2017; 81: 432-440.

24) Mocco J, Brown RD Jr, Torner JC, Capuano AW, Fargen KM, Raghavan ML, Piepgras DG, Meissner I, Huston J III; International Study of Unruptured Intracranial Aneurysms Investigators. Aneurysm morphology and prediction of rupture: an international study of unruptured intracranial aneurysms analysis. Neurosurgery 2017; 82: 491-496.

25) Laaksamo E, Tulamo R, Baumann M, Dashti R, Hernesniemi J, Juvela S, Niemelä M, Laakso A. Involvement of mitogen-activated protein kinase signaling in growth and rupture of human intracranial aneurysms. Stroke 2008; 39: 886-892.